The stable molten globule

Under mild denaturing conditions several, but by no means all, proteins take up a partially denatured conformation having the following characteristics:

- condensed, with a Stokes radius equal to or not much greater than that of the folded protein
- exhibiting substantial secondary structure, indicated by the far-UV CD spectrum, but with generally reduced stability of the constituent hydrogen bonds
- many side-chains have lost the persistent tertiary interactions of the N state
- the molecule behaves as if 'sticky', consistent with a degree of exposure of non-polar groups to solvent
- if the folded protein is an enzyme, the intermediate is inactive
- an equilibrium transition to the unfolded state suggesting a degree of co-operativity

FIGURE 6–6. Schematic representation of the native and the molten globule states of protein molecules. Nonpolar side chains are hatched.

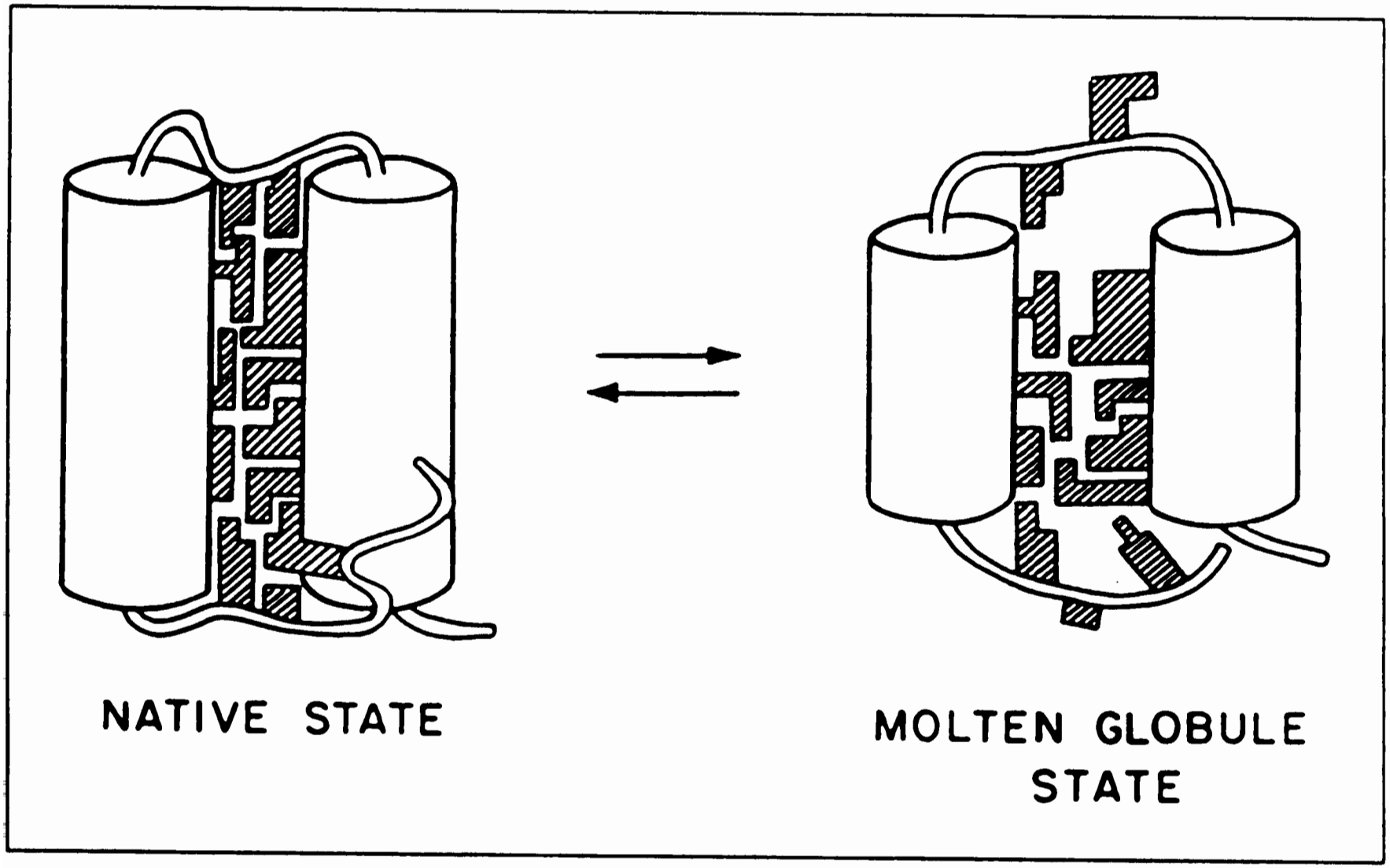

FIGURE 6–6. Schematic representation of the native and the molten globule states of protein molecules. Nonpolar side chains are hatched.

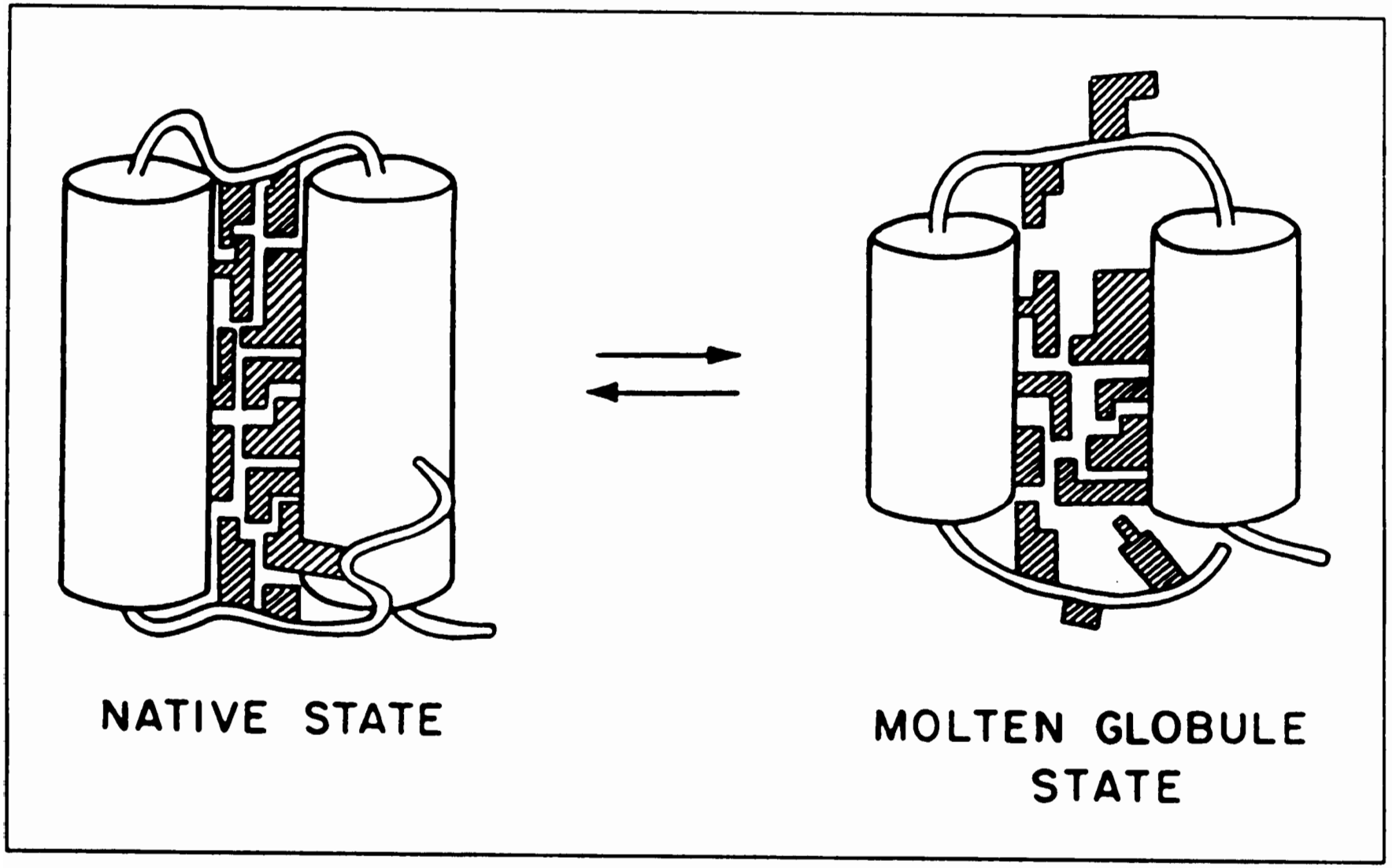

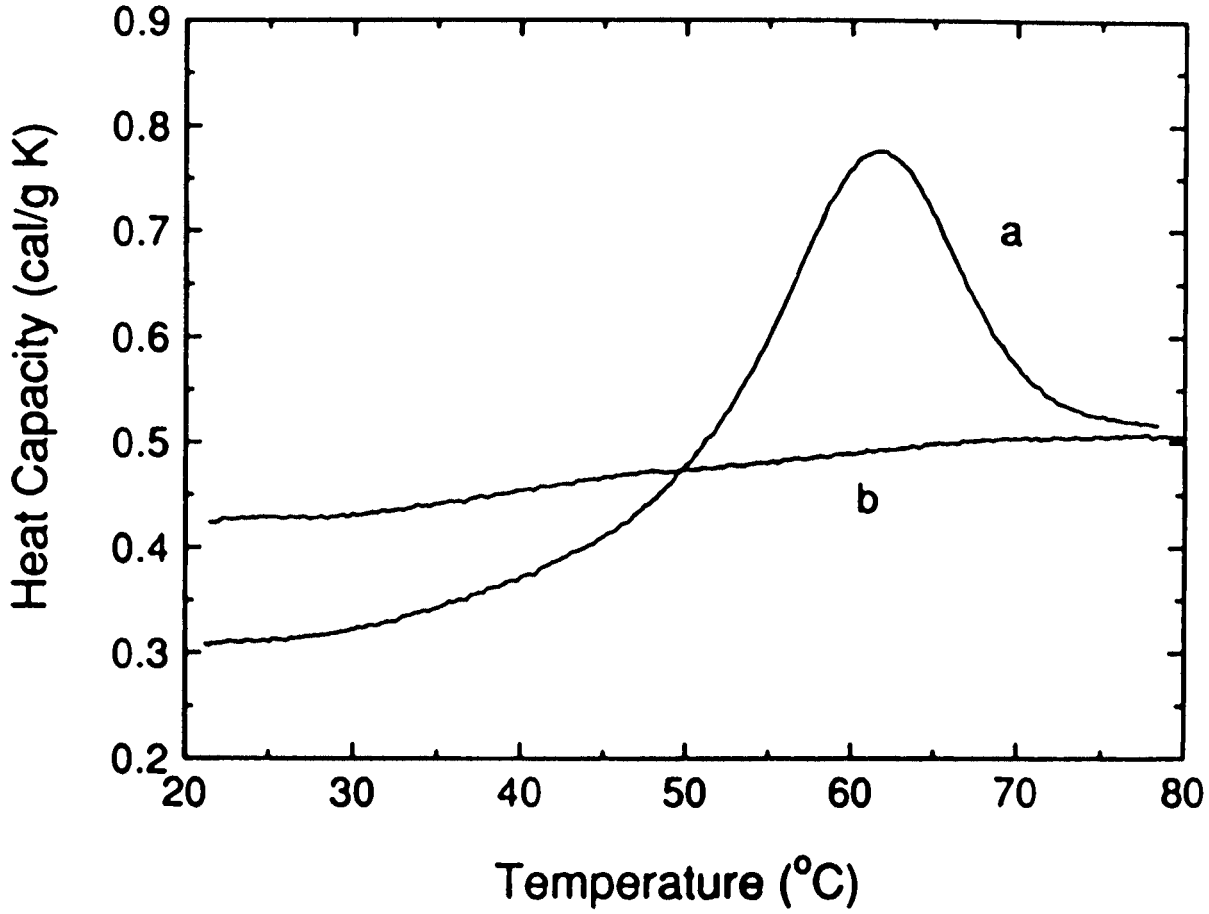

Figure 1. Heat capacity curves of holo-α-lactalbumin and apo-α-lactalbumin. Calorimetry was carried out with DASM4 at the scan rate of 1·0 K/min. Each curve obtained after subtraction of the curve for the dialysis buffer solution as a reference. Curve a: holo-α-lactalbumin (2·14 mg/ml) after dyalisis against 10 mM-borate buffer (pH 8·0). The pH of the solution after heating was 7·8. Curve b: apo-α-lactalbumin (2·48 mg/ml) after dialysis against 10 mM-borate buffer containing 1 mM-EGTA (pH 8). The pH of the solution after heating was 7·6.

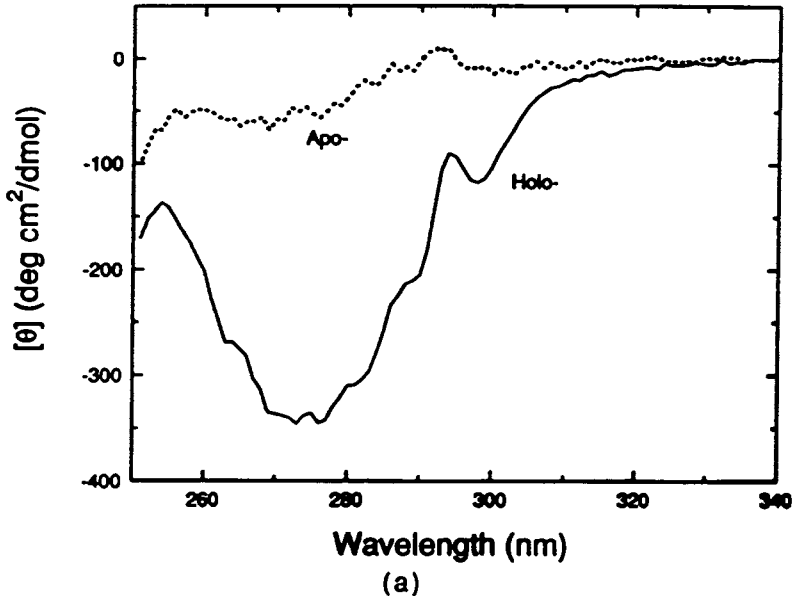

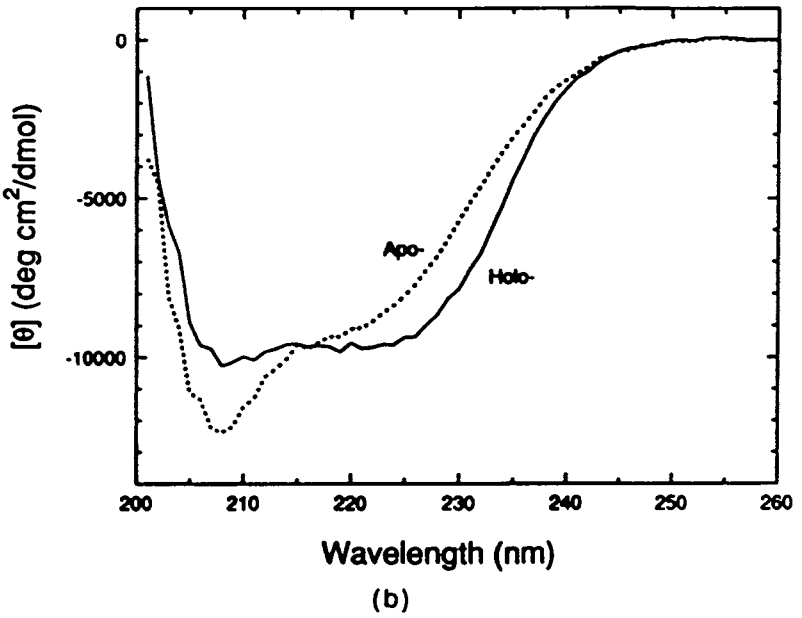

Figure 2. Circular dichroism spectra of holo-α-lactalbumin and apo-α-lactalbumin in the aromatic and far-u.v. regions at 25°C. The c.d. spectra were scanned 16 times at the scan rate of 20 nm/min using a 0·25 s time constant with a Jasco J-500, and the spectra were averaged. For calculation of the mean residue ellipticity, θ, the mean residue weight was taken at 115 for both the proteins. (a) c.d. spectra in the aromatic region were measured at protein concentrations of 0·76 mg/ml for both holo-α-lactalbumin and apo-α-lactalbumin, using a cell with a 10 mm light-path length. The same samples as those for calorimetry were diluted with dialysis buffer. The solutions were at pH 7·7 for holo-protein and at pH 7·6 for apo-protein. (b) c.d. spectra in the far-u.v. region were measured at protein concentrations of 0·41 mg/ml for holo-α-lactalbumin and 0·49 mg/ml for apo-α-lactalbumin, using a cell with a 1 mm path length. The same samples as those for calorimetry were diluted with dialysis buffer. The solutions were at pH 7·5 for holo-protein and at pH 7·6 for apo-protein.

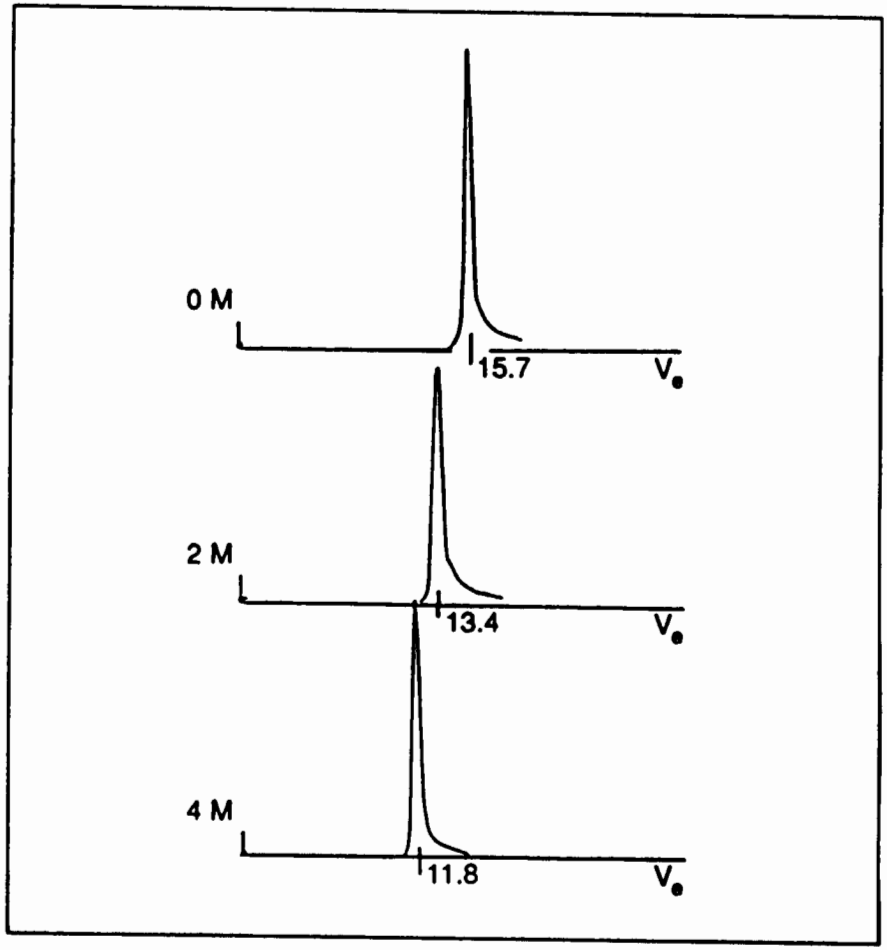

Fig. 2. Size determination of a stable molten globule. Elution profiles are shown for β-lactamase applied in buffer containing the stated concentrations of urea (23). At 2 M urea the protein exhibits the properties of a molten globule (H) and at 4 M is unfolded (U) (14). The values of the elution volume, V_e, are in ml.

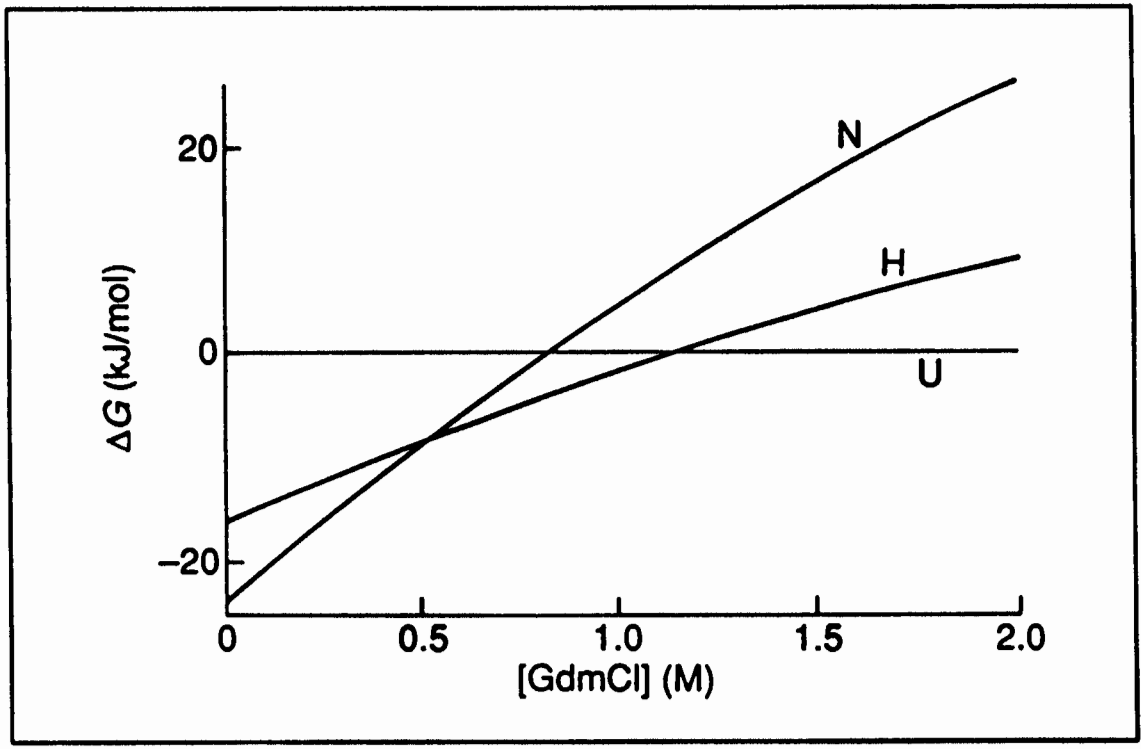

Fig. 5. The free energies of stabilization of the native and intermediate conformers as a function of denaturant concentration. From the three-state denaturation transitions for β-lactamase the free energy differences (equilibrium constants) between the forms were calculated and plotted for the native (N) and molten globule (H) forms, both relative to the unfolded state (35).

The kinetic molten globule

It has been known for a long time that, while native activity and aromatic residue environment frequently recover relatively slowly on refolding, far-UV ellipticity is regained rapidly (35). This points to the accumulation during folding of an intermediate containing secondary structure. Such an intermediate, usually termed I (15, 36), has been identified as the one that precedes the main energy barrier and rate-limiting step in folding:

$$U \xrightarrow{\text{fast}} I \xrightarrow{\text{slow}} N.$$

This intermediate has been the subject of much subsequent research—and discussion!—in the field of protein folding. It has been shown experimentally to:

- be condensed
- contain secondary structure
- have few persistent tertiary interactions
- be 'sticky'
- be inactive (for enzymes)
- be transient, preceding the main rate-limiting step in folding.

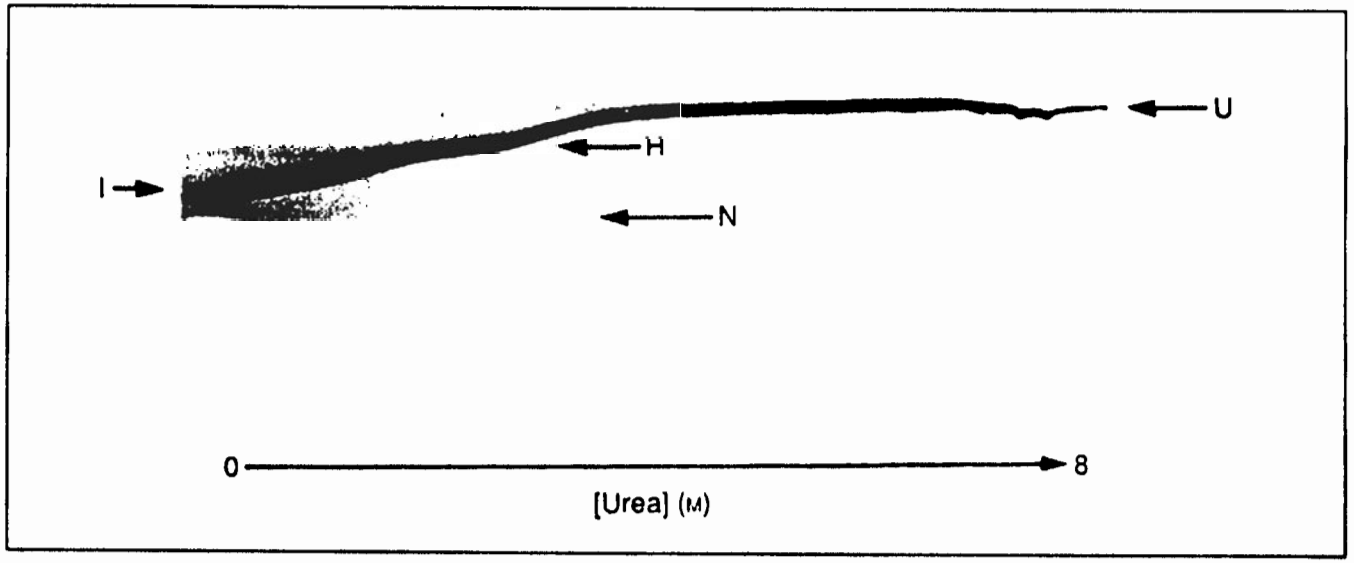

Fig. 6. Characterization of folding intermediates by urea gradient gel electrophoresis. β-lactamase dissolved in 2M urea (i.e. in the molten globule, H, state) was applied across the gradient of urea and, after electrophoresis downwards, detected by Coomassie blue staining (15). Smooth transition curves show that the stable molten globule, H, is in fast equilibrium with the unfolded state, U, and with an even more compact intermediate, I, at urea concentrations in which the protein folds to the active enzyme, N. Since both U and H are known to fold slowly to N, I accumulates rapidly during folding and undergoes a slow transition to N, indicated by the separation between the bands for I and N.

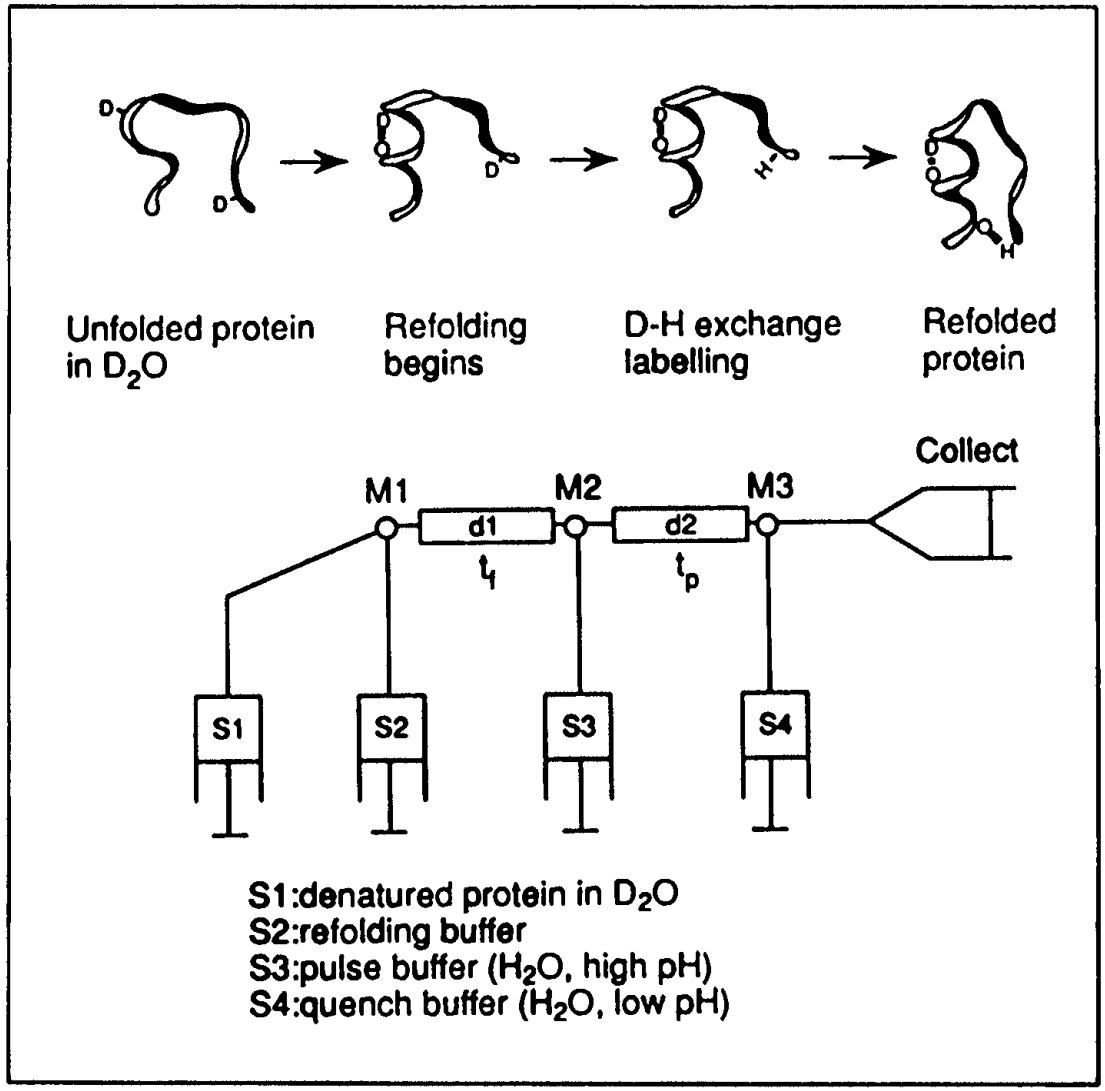

Fig. 1. Schematic illustration of the pulsed hydrogen exchange method. The basic principle is illustrated (*top*) with a hypothetical 'protein' with two representative amide probes. The first ND group becomes protected against exchange in a rapidly forming helical hydrogen bond and remains deuterated, while the second one is still exposed at this time and becomes protonated by D to H exchange during the labelling pulse. A diagram of a quenched-flow apparatus with three mixing stages (M1–M3) and two variable delay lines (d1 and d2) is shown (*below*). Syringes S1 and S2 are activated at t = 0 to initiate refolding by dilution of the denaturant in mixer M1. After a refolding time t_f, the protein solution is mixed in M2 with an H_2O buffer at basic pH (typically pH 9–10) to start the D to H exchange reaction. After a pulse time t_p, exchange is quenched by lowering the pH in M3 under conditions that favour rapid refolding.

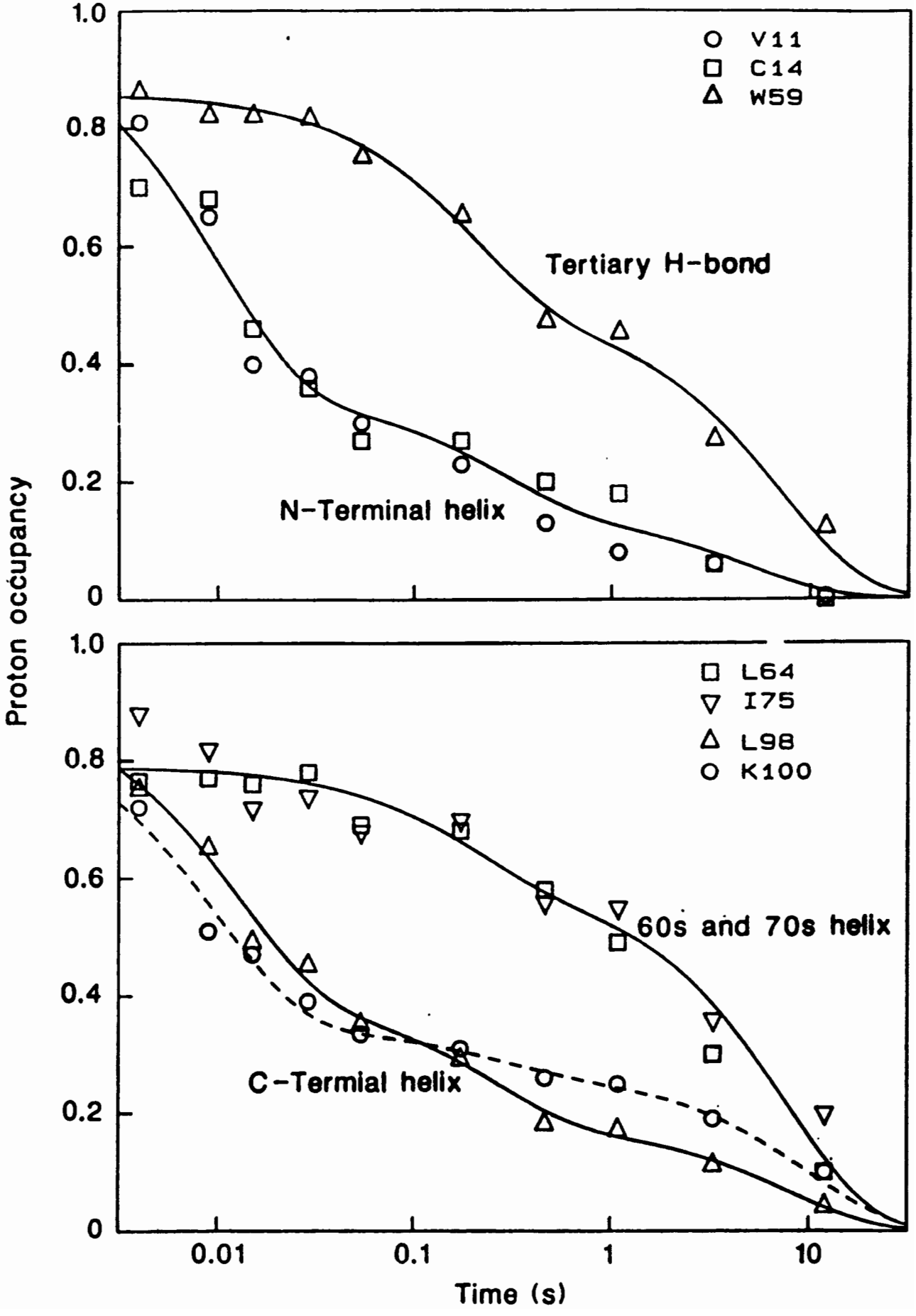
1.0
0.8
0.6
0.4
0.2
0
Proton occupancy
V11
C14
W59
Tertiary H-bond
N-Terminal helix
L64
I75
L98
K100
60s and 70s helix
C-Termial helix
0.01
0.1
1
10
Time (s)

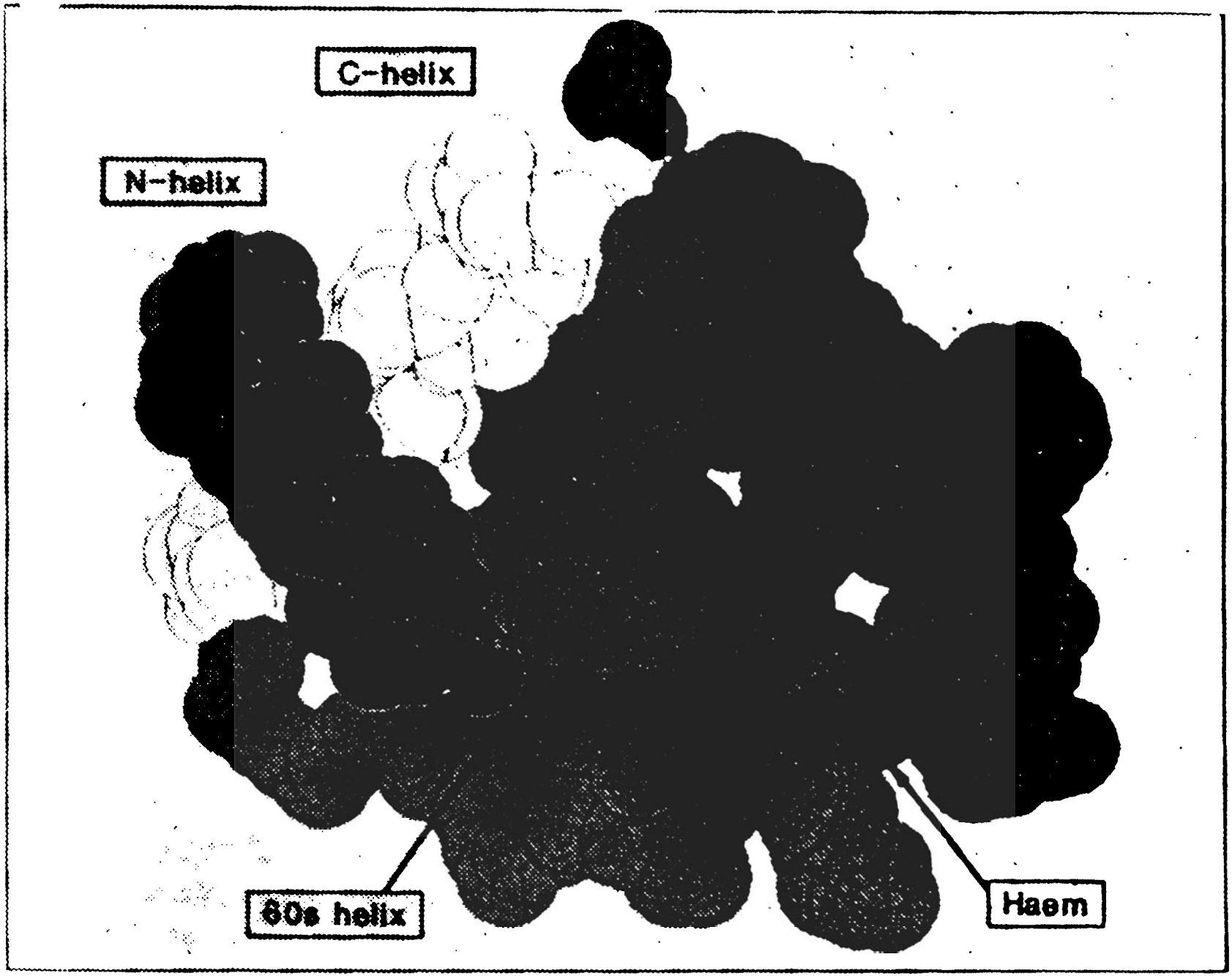

Space-filling model of cytochrome *c*

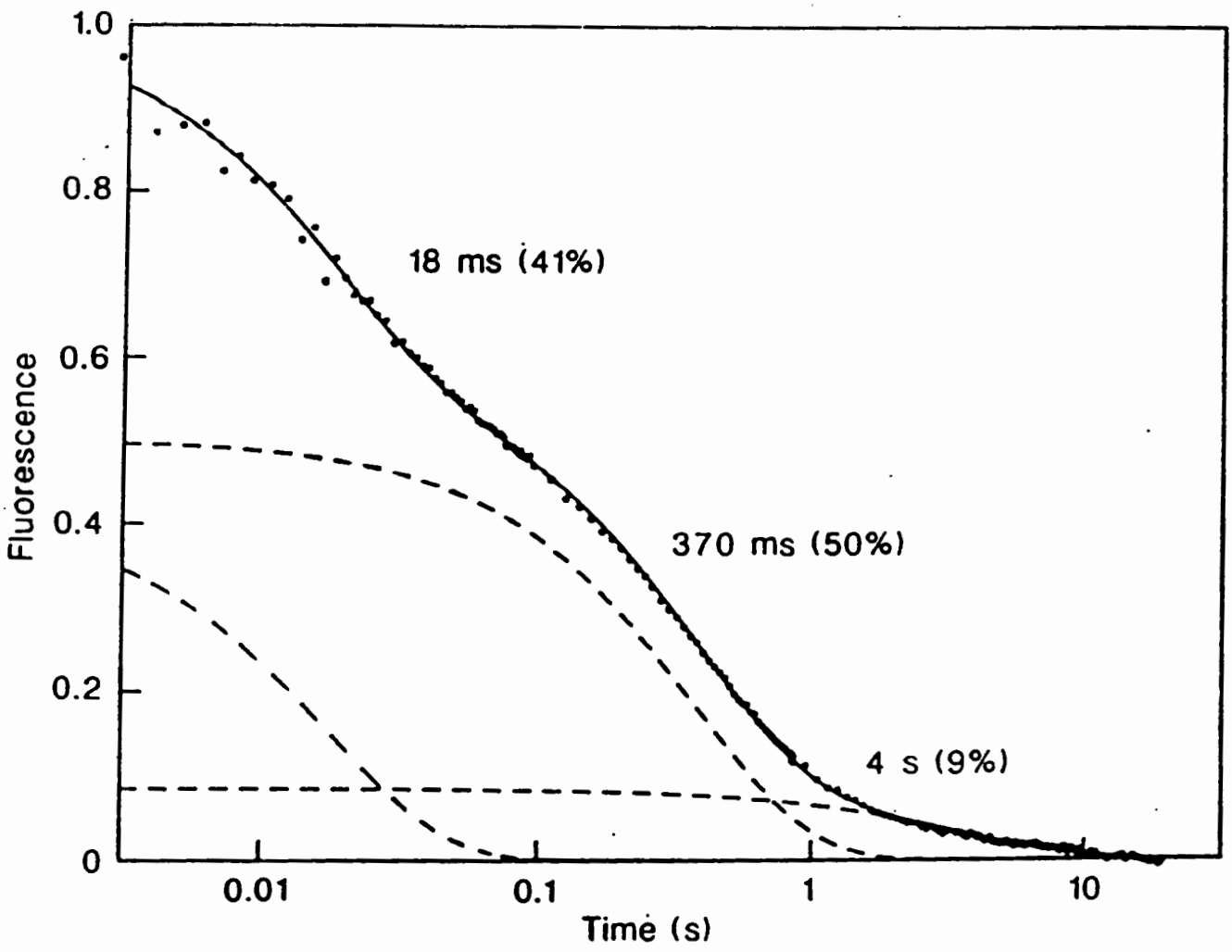

Fig. 4 Refolding kinetics in cytochrome *c* at 10 °C, monitored by the fluorescence of a single tryptophan residue (Trp 59). The data were collected on a Hi-Tech stopped-flow apparatus, using a deuterium lamp for excitation at 280 nm and observation of the fluorescence emission at 350 nm. As in the pulse labelling experiments (Fig. 1), cytochrome *c* was unfolded in 4.2 M GuHCl, *p*H 6.0, and refolded at *p*H 6.2 in the presence of 0.7 M GuHCl. The final protein concentration was 5×10^{-6} M. Under these conditions, unfolding was fully reversible. The kinetic data are presented on the same logarithmic timescale used in Fig. 3. The solid curve was obtained by nonlinear least-squares fitting of three exponential phases, resulting in the indicated time constants and amplitudes. The individual phases are displayed separately with dashed lines.

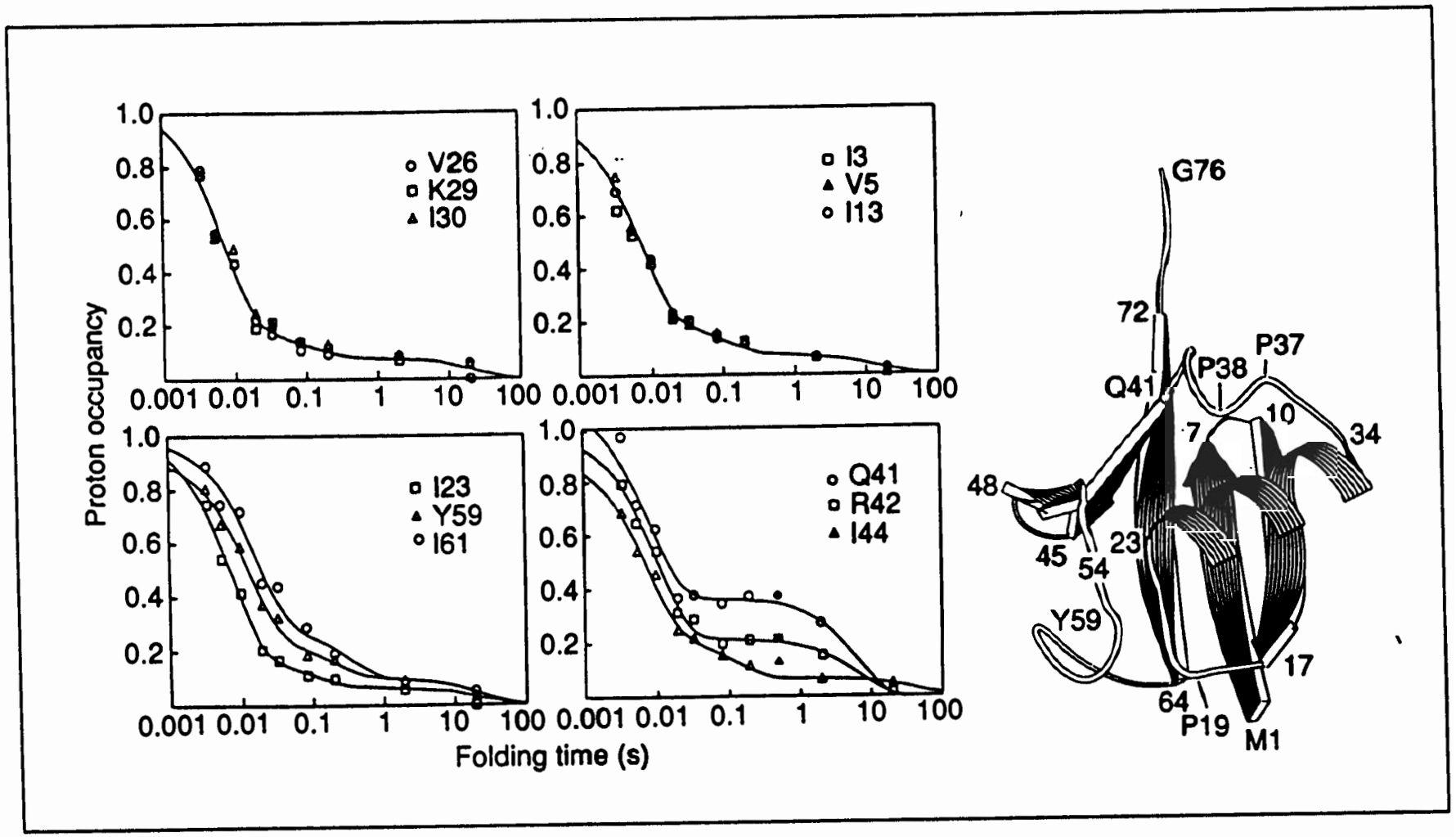

Fig. 6. Time course of amide protection in the folding reaction of ubiquitin (25 °C, pH 5), measured by pulsed hydrogen exchange (75). The proton occupancies for representative amide probes are plotted versus refolding time on a logarithmic scale (1 ms to 100 s). The ribbon diagram shows the backbone structure of ubiquitin. Adapted from ref. 75.

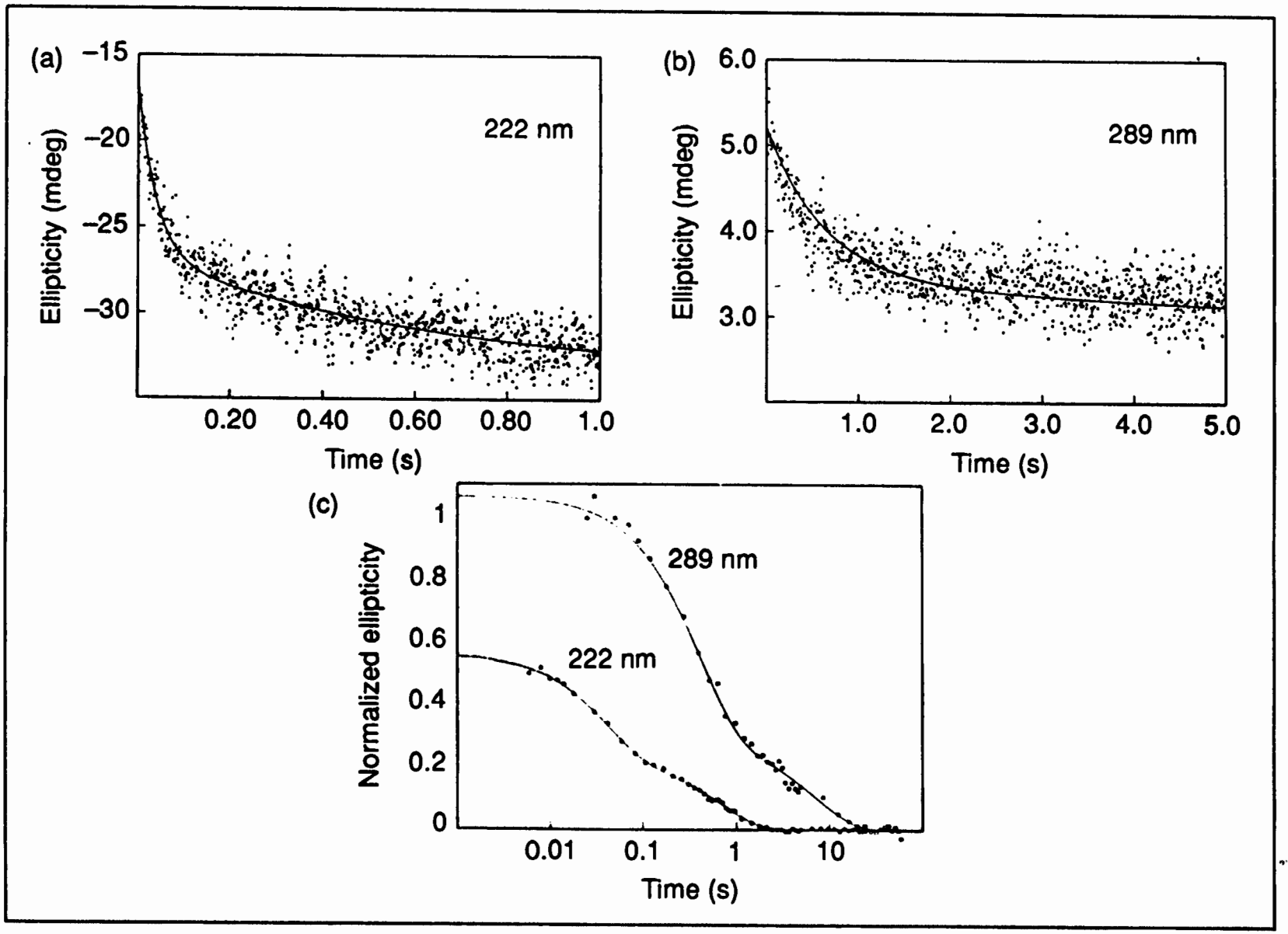

Fig. 3. CD-detected stopped-flow folding kinetics for oxidized cyt *c* at pH 6.3, 10 °C, monitored at 222 nm (a) and 289 nm (b). The folding kinetics at both wavelengths are compared in (c), which shows plots of the normalized ellipticity relative to the fully unfolded state on a logarithmic time-scale. Reprinted from ref. 73, with permission.

Table 1 Relative amplitudes of 'burst phase' measured by time-resolved far-UV CD spectroscopy for various globular proteins

Protein	Amplitude (%)[a]	Dead time (ms)	Reference
α-Lactalbumin	50	20	69
β-Lactoglobulin	200	18	17
Chymotrypsinogen A	100	18	116
Cytochrome *c*	44	4	73
Dihydrofolate reductase	40	18	96
Hen lysozyme	90	4	65,92
Parvalbumin	60	18	97
Rat intestinal fatty acid binding protein	32	~100	115
Ribonuclease T1	100	15	116
Staphylococcal nuclease A	30	15	114
Tryptophan synthase β2	57	13	117
Tryptophan synthase β2 (F2–V8 fragment)	100	4	118

[a] The burst phase amplitude represents the % change in the far-UV CD signal (216–225 nm) occurring in the dead time of the stopped-flow experiment relative to the total change upon refolding.

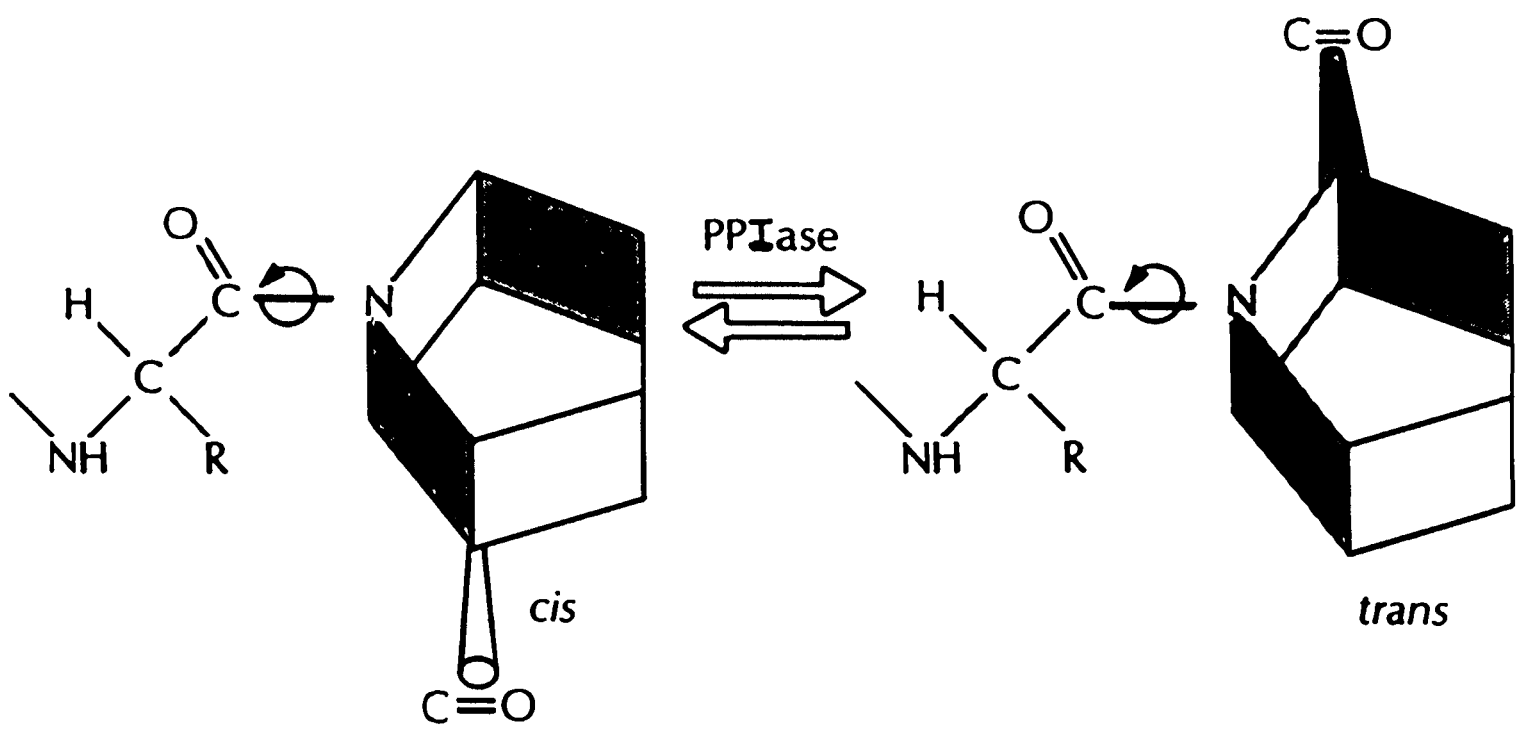
O
H
C
N
NH
R
C=O
cis
PPIase
O
H
C
N
NH
R
C=O
trans

Thiol–disulfide chemistry

Chemical reactions in the formation and trapping of disulfide-bonded folding intermediates. **(a)** Thiol-disulfide exchange between a protein thiolate and a reagent disulfide (RS-SR) to generate a mixed disulfide. **(b)** Intramolecular thiol-disulfide exchange between a protein thiolate and a mixed disulfide which generates a protein disulfide. **(c)** Intramolecular thiol-disulfide exchange between a protein thiolate and an existing protein disulfide to generate a different protein disulfide. **(d)** Protonation of a protein thiolate to generate an unreactive thiol. **(e)** Alkylation of a protein thiol by iodoacetate.

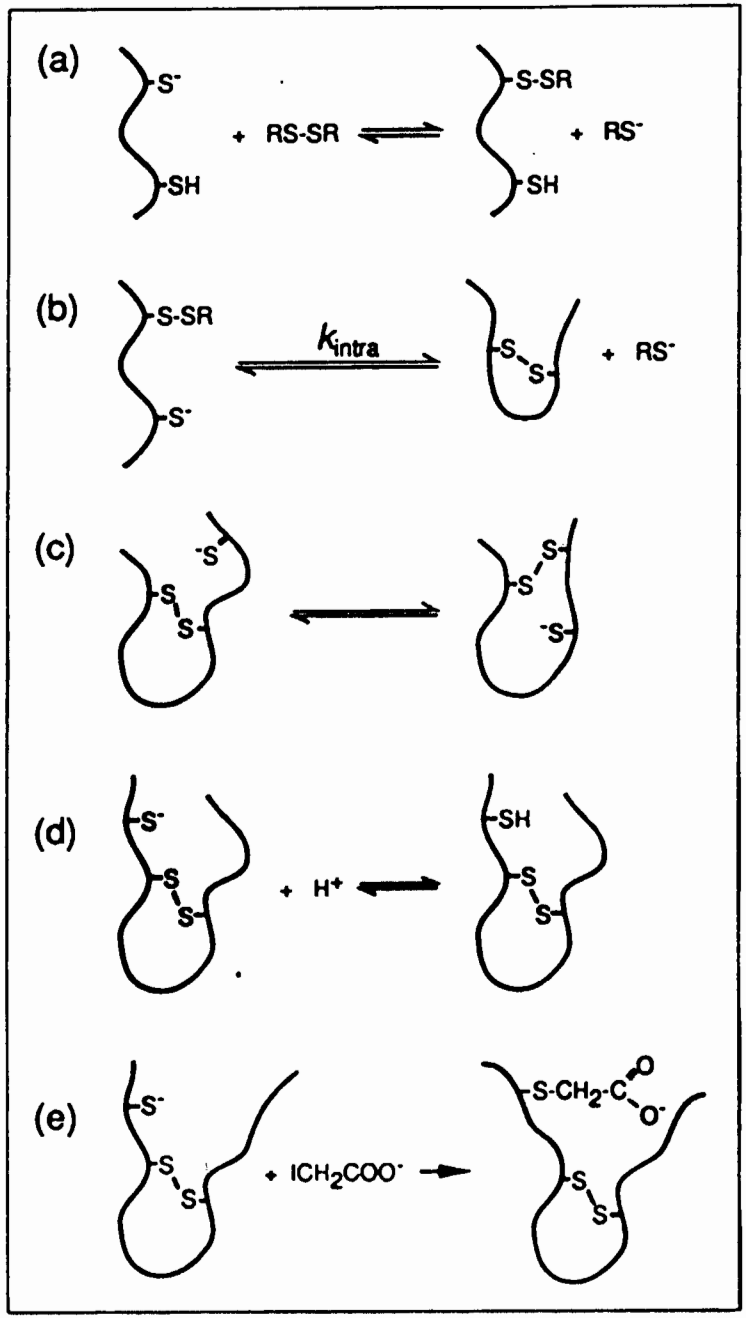

Thiol/disulfide exchange

Disulfide bond formation from two thiols is a two electron oxidation reaction that requires an oxidant. While molecular oxygen (in the presence of trace amounts of heavy metals) may adequately serve this role for some proteins, the most common source of oxidizing equivalents is a low molecular weight disulfide. Protein thiol oxidation to the disulfide results from a thiol/disulfide exchange process (10) that transfers oxidizing equivalents from the low molecular weight disulfide to the protein (eqn 1).

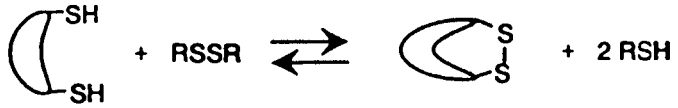

[1]

Thiol/disulfide exchange occurs via direct attack of a nucleophilic thiolate anion on one of the sulfurs of the disulfide bond (eqn 2) (11, 12). The transition state is rather symmetrical with approximately equal bond formation to the nucleophilic sulfur (R_nS^-) and the leaving sulfur ($R_{lg}S^-$) and with a relatively small amount of negative charge on the central sulfur (R_cS) (13).

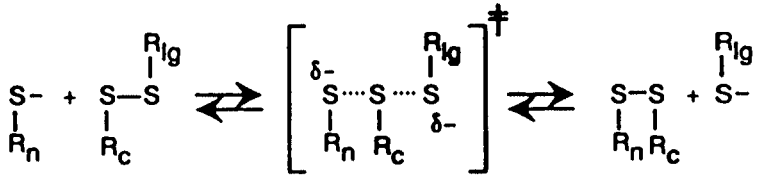

[2]

The rate constant for the reaction increases as the basicity of the attacking thiolate (R_nS^-) nucleophile increases (pK_a increases) and as the basicity of the leaving thiolate ($R_{lg}S^-$) decreases (pK_a decreases). The pK_a of the typical cysteine sulfydryl group is about 8.6; however, this may vary considerably from protein to protein due to the effects of the local environment. At a pH of 8.6, the typical intermolecular step of thiol/disulfide exchange between small molecules or unhindered protein thiols and disulfides will occur with a second-order rate constant of about 20 M^{-1} s^{-1} (14). Since thiol/disulfide exchange occurs via the attack of a nucleophilic thiolate anion, the rate will increase with increasing pH until the attacking thiol is predominantly in the thiolate form.

Protein Disulfide-Isomerase (PDI) accelerates the exchange reactions between disulfide bonds in proteins in the presence of appropriate oxidizing or reducing reagents.

Reaction:

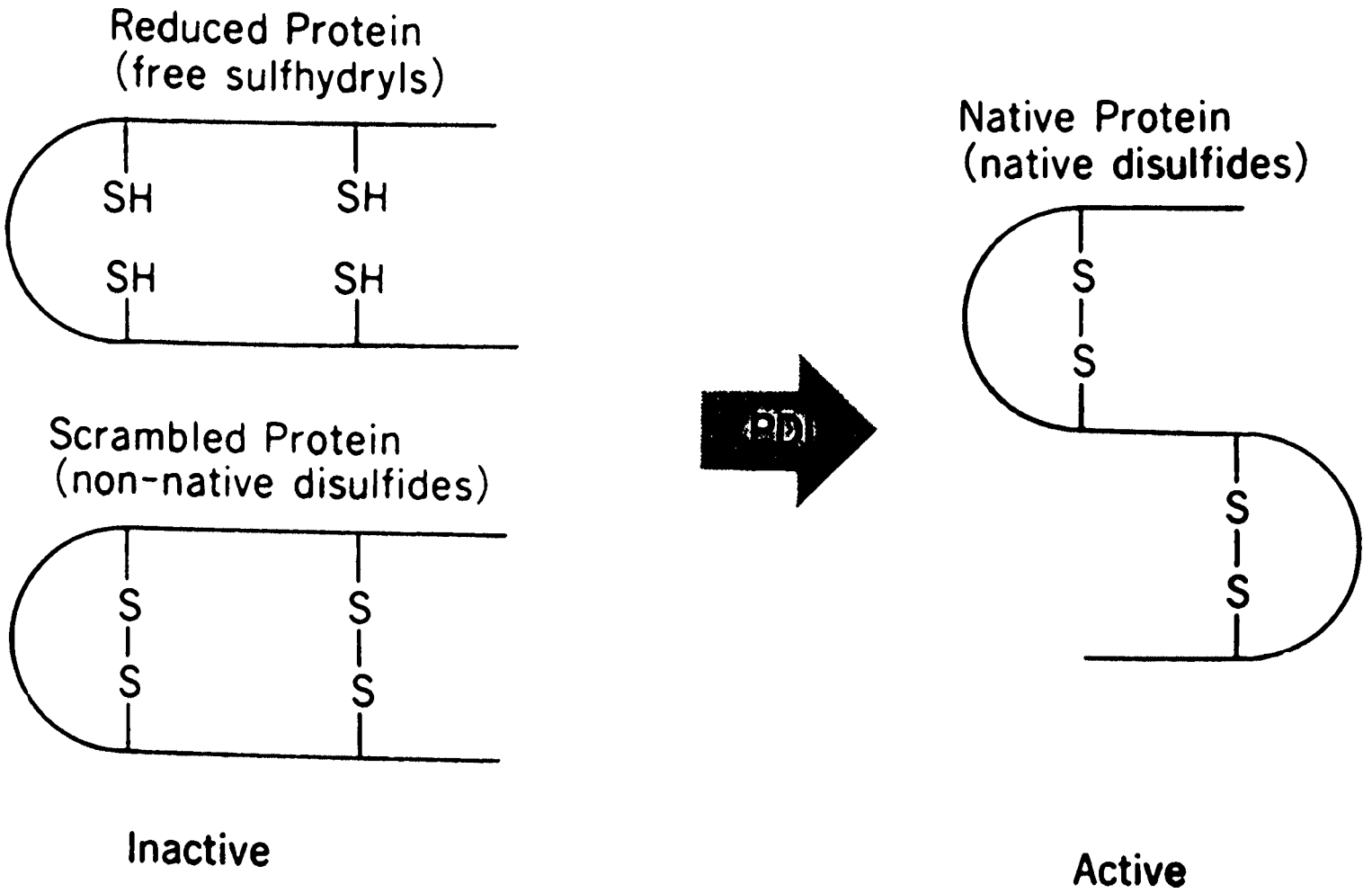

Refolding System

	final conc.
Substrate protein	200 μg/ml
Sodium phosphate buffer, pH 7.5	100 mM
Glutathione	0.2 mM
Reduced glutathione	2 mM
PDI	20 μg/ml

Results

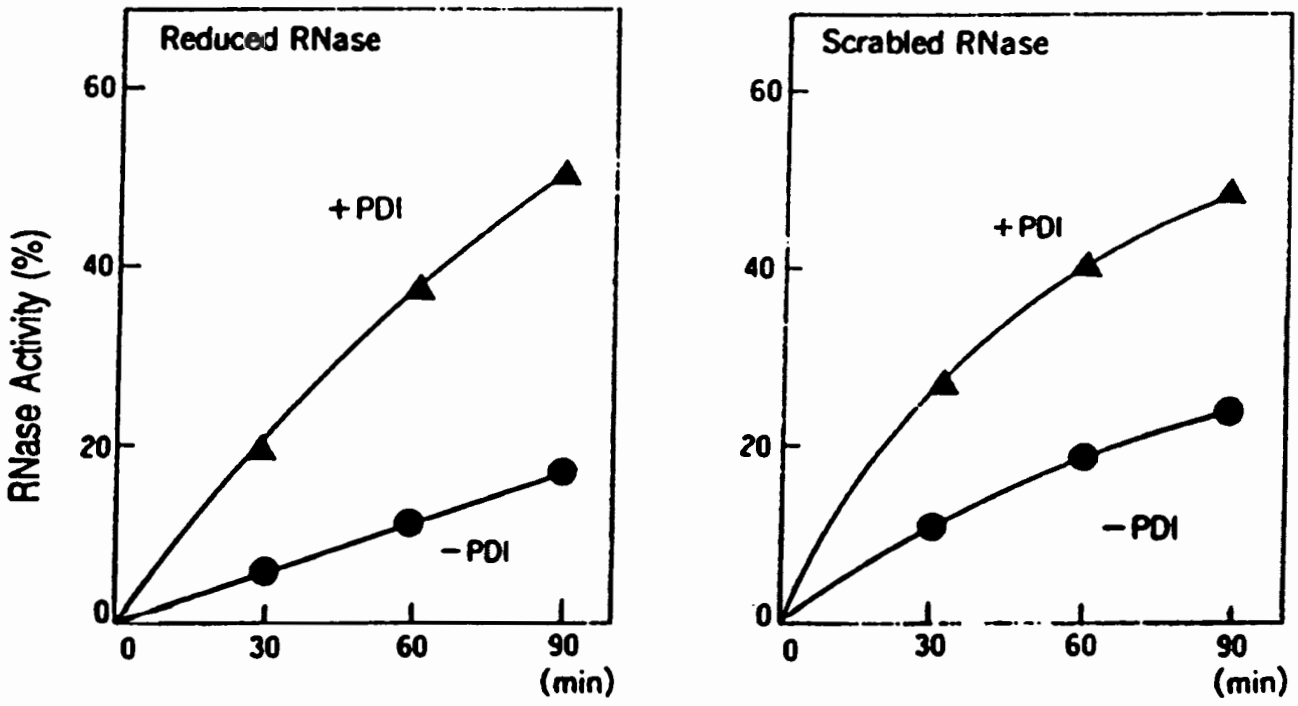

Table 1 Chaperone proteins and their known functions in the cell.

Subcellular location	Organism	Component	Subunit M_r (kDa)	Known functions
The hsp 70 family				
Cytosol	*E. coli*	DnaK	69	Co-operation with the heat shock proteins DnaJ and GrpE in λ DNA replication; activation of RepA for binding to *ori*P1 DNA (86–88); dissociation of protein aggregates (90)
	Yeast	Ssa1–4p	69–72	Stabilization of precursor proteins for translocation into ER and mitochondria (38, 71); binding to nascent polypeptides (72)
	Mammals	hsc70		Uncoating of clathrin-coated vesicles (91)
Mitochondria	Yeast	Ssc1p	70	Membrane translocation, folding of imported proteins (73, 75)
Endoplasmic reticulum	Yeast	Kar2p	78	Protein translocation into the ER; assembly within the ER (31); retention of misfolded proteins (29, 79)
		BiP, Grp78	70	
The hsp60 family				
Cytosol	*E. coli*	GroEL	58	Folding of monomeric and multi-subunit proteins (102, 103, 109–113, 116, 118)
		GroES	10	
Mitochondrial matrix	Fungi, mammals	hsp60, hsp58	58–64	Folding and assembly of newly imported proteins (75, 101)
		hsp10	10	
Chloroplasts	Plants	Rubisco subunit binding protein	61 (α-chain) 60 (β-chain)	Folding and assembly of rubisco and probably of other proteins imported into chloroplasts (151)
SecB	*E. coli*		17	Stabilization of precursor proteins for export across the cytoplasmic membrane (45, 127)
The hsp90 family				
Cytosol	Mammals	hsp90	90	Stabilization of steroid hormone receptors in a conformation competent to bind hormone (139); association with $pp60^{src}$ before its phosphorylation (134); facilitation of refolding by preventing aggregation (143)

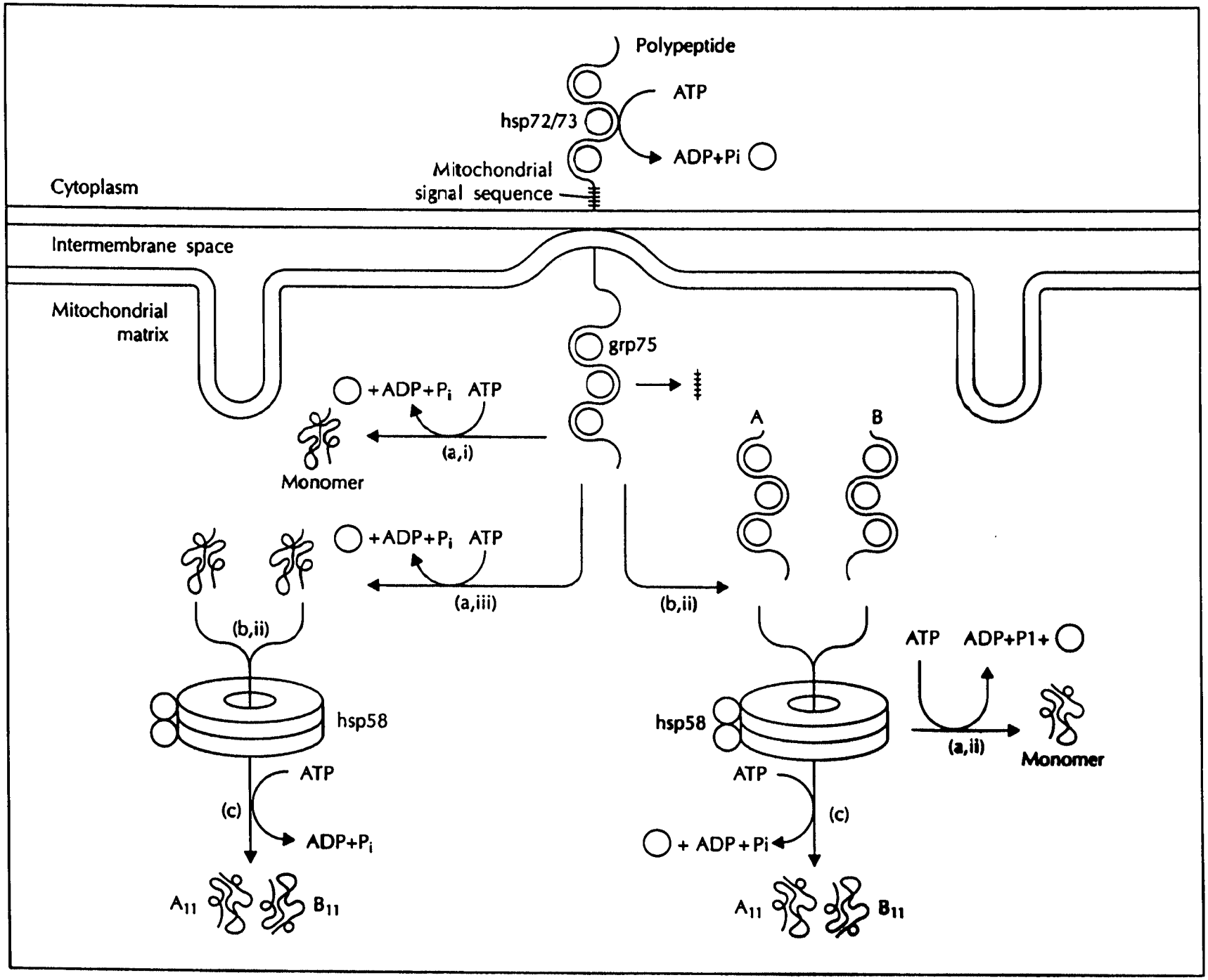
Polypeptide
ATP
hsp72/73
ADP+Pi
Mitochondrial
signal sequence
Cytoplasm
Intermembrane space
Mitochondrial
matrix
grp75
+ADP+Pi ATP
(a,i)
Monomer
A
B
+ADP+Pi ATP
(a,iii)
(b,ii)
(b,ii)
ATP ADP+P1+
hsp58
hsp58
(a,ii)
Monomer
ATP
ATP
(c)
(c)
ADP+Pi
+ ADP+Pi
A11
B11
A11
B11

'The *in vivo* folding problem', or 'Out of the ribosome, into the jungle'